Characterization of the Intracellular Calcium Store at the Base of the Sperm Flagellum That Regulates Hyperactivated Motility[1]

Han-Chen Ho and Susan S. Suarez[2]

Department of Biomedical Sciences, College of Veterinary Medicine, Cornell University, Ithaca, New York 14853

ABSTRACT

Hyperactivated sperm motility is usually characterized by high-amplitude flagellar bends and asymmetrical flagellar beating. There is evidence that an inositol 1,4,5-trisphosphate (IP$_3$) receptor-gated Ca^{2+} store in the base of the flagellum provides Ca^{2+} to initiate hyperactivation; however, the identity of the store was not known. Ca^{2+} stores are membrane-bounded organelles, and the only two membrane-bounded organelles found in this region of sperm are the redundant nuclear envelope (RNE) and mitochondria. Transmission electron micrographs revealed two different compartments of RNE, one enriched with nuclear pores and the other containing few pores but extensive membranous structures with enlarged cisternae. Immunolabeling showed that IP$_3$ receptors and calreticulin are located in the region containing enlarged cisternae. In other cell types, mitochondria adjacent to Ca^{2+} stores are actively involved in modulating Ca^{2+} signals by taking up Ca^{2+} released from stores and also may respond by increasing production of NADH and ATP to support increased energy demand. Nevertheless, bull sperm did not show an increase in NADH when Ca^{2+} was released from intracellular stores by thapsigargin to induce hyperactivation. Consistently, no net increase in ATP production was detected when sperm were hyperactivated, although ATP was hydrolyzed at a greater rate. Furthermore, blocking Ca^{2+} efflux from mitochondria by CGP-37157, a specific inhibitor of the mitochondrial Na$^+$/Ca^{2+} exchanger, did not inhibit the development of hyperactivated motility. We concluded that the intracellular Ca^{2+} store is the part of RNE that contains enlarged cisternae and that Ca^{2+} is released directly to the axoneme to trigger hyperactivated motility without the active participation of mitochondria.

calcium, fertilization, gamete biology, sperm motility and transport

INTRODUCTION

Hyperactivation is a movement pattern shown by sperm at the site and time of fertilization in mammals [1, 2]. It is usually characterized by high amplitude, asymmetrical flagellar beating and is known to be regulated by Ca^{2+} [3]. There is evidence that an inositol 1,4,5-trisphosphate (IP$_3$) receptor-gated Ca^{2+} store in the base of the flagellum is involved in releasing Ca^{2+} to the axoneme to initiate sperm hyperactivated motility [4]; however, the identity of the store is not known.

Ca^{2+} stores are membrane-bounded organelles, such as endoplasmic and sarcoplasmic reticula. The only two membrane-bounded organelles found in the neck region of sperm are the redundant nuclear envelope (RNE) and mitochondria [5].

The RNE evolves during spermiogenesis when condensation of nuclear chromatin leaves excess nuclear envelope [6]. It was named the redundant nuclear envelope because it was believed to lack physiological functions. Nevertheless, the RNE is not shed during sperm maturation, as are other useless organelles, but instead is packaged into the neck region. Furthermore, RNEs are retained in a wide variety of mammals, including mice [7], hamsters [3], monkeys [6], bats [8], bulls [9], and humans [10]. These observations indicate that RNE does serve a function, and we propose that it serves as a Ca^{2+} store. There is physiological evidence that nuclear envelopes serve as Ca^{2+} stores in other cell types. Nuclear envelopes in hepatocytes release Ca^{2+} in response to IP$_3$ [11], while those in starfish oocytes release Ca^{2+} in response to IP$_3$ and ryanodine [12].

The only other membrane-bounded organelles in the neck region of sperm are the initial mitochondria of the helix of mitochondria that wraps around the axoneme throughout the midpiece of the flagellum. IP$_3$ receptors have never been reported to exist in mitochondria; however, mitochondria have been found strategically localized near Ca^{2+} stores such that Ca^{2+} released from the store is rapidly transported into the mitochondrial matrix [13]. Rizzuto et al. [14] demonstrated that mitochondria in HeLa cells are closely associated with endoplasmic reticulum (ER) and pick up Ca^{2+} released from the ER stores immediately after stimulation. The coupling between increases in cytosolic Ca^{2+} concentration and mitochondrial matrix Ca^{2+} concentration has been proposed to coordinate mitochondrial ATP production with cellular energy demand [15]. Upon induction of hyperactivation in bull sperm, Ca^{2+} increases in the neck region, then rapidly propagates down the flagellar midpiece [4]. When bull sperm are demembranated by detergent and then reactivated, more ATP must be provided (along with additional Ca^{2+}) to support hyperactivation than is required for activation [16]. These observations indicate that the mitochondria of the midpiece could take up the Ca^{2+} and respond by increasing ATP production for hyperactivation.

The arrangement of RNE and mitochondria at the base of the flagellum and the requirement of increased Ca^{2+} and ATP for hyperactivation led us to test the following hypothetical model: the RNE serves as a Ca^{2+} store that provides increased Ca^{2+} to the axoneme and the mitochondria and the mitochondria are stimulated by Ca^{2+} release to increase ATP production.

MATERIALS AND METHODS

Media and Chemicals

A modified Tyrode balanced salt solution (TALP, consisting of 99 mM NaCl, 3.1 mM KCl, 25 mM NaHCO$_3$, 0.4 mM NaH$_2$PO$_4$, 1.1 mM MgCl$_2$,

2 mM $CaCl_2$, 10 mM Hepes, 1 mM pyruvate, 25.4 mM lactate, 50 μg/ml gentamycin, and 6 mg/ml Fraction V BSA, pH 7.45, 290–300 mOsm/kg), sterilized through a 0.22-μm Nalgene cellulose acetate filter (Nalge Co., Rochester, NY), was used for washing and incubating sperm. TALP was equilibrated in a humidified atmosphere at 39°C containing 5% CO_2 before use.

Chemicals were purchased from Sigma-Aldrich Co. (St. Louis, MO) with the exception of those noted here. BSA, Hepes, thapsigargin, and ATP assay kit were from Calbiochem Corporation (La Jolla, CA). Glutaraldehyde, osmium tetroxide (OsO_4), sodium cacodylate, uranyl acetate, lead citrate, LR white, and LR gold embedding media were from Electron Microscopy Sciences (Fort Washington, PA). Fluo-3FF acetoxymethyl (AM) ester was from Teflabs (Austin, TX).

Sperm Preparation

Semen was generously donated by Genex Cooperative, Inc. (Ithaca, NY). Fresh ejaculated bull semen was diluted 1:5 with TALP immediately after collection and transported to the laboratory in a 39°C water bath (bovine body temperature) for use within about 60 min. Sperm were washed free of diluted seminal plasma by centrifuging twice in fresh TALP at 170 × g for 10 min each. Washed sperm were adjusted to 40 × 10^6/ml in TALP and kept at 39°C under 5% CO_2 for the duration of the experiment.

Indirect Immunofluorescence Labeling

Washed ejaculated bull sperm (100 μl, 10^8 sperm/ml) were fixed with 1 ml 1% formaldehyde in PBS at room temperature for 15 min. The action of formaldehyde was stopped by adding 14 ml of 0.2 M glycine. Fixative and glycine were discarded after centrifuging the sperm at 500 × g for 10 min. The sperm pellet was resuspended in PBS to 10^7 sperm/ml, then 10 μl of sperm suspension were dried down in each well of a Teflon-coated slide (Electron Microscopy Sciences, Fort Washington, PA). After rinsing the slides with PBS, 10 μl of 0.1% Triton X-100 were added to each well for 15 min to permeabilize the sperm membranes. Slides were then rinsed and treated with 3% BSA in PBS for 30 min to block nonspecific binding. For IP_3 receptor localization, the permeabilized sperm were probed with affinity-purified polyclonal rabbit antibody, produced against a synthetic peptide consisting of the 15 C-terminal amino acids of rabbit brain IP_3 receptor [17]. Controls were incubated with preimmune serum. Antibody binding was visualized using fluorescein isothiocyanate (FITC)-conjugated goat anti-rabbit IgG (1:200 dilution; Sigma-Aldrich). To detect nuclear pores, permeabilized bull sperm were probed with mouse monoclonal antinuclear pore complex antibody (1:500 dilution, mAb 414; BabCo, Berkeley, CA) [18] and the labeling was visualized by tetramethylrhodamine isothiocyanate (TRITC)-conjugated goat anti-mouse IgG (1:200 dilution; Sigma-Aldrich). Anti-calreticulin polyclonal rabbit antibody (1:150 dilution; Novus Biologicals, Inc., Littleton, CO) and FITC-conjugated goat anti-rabbit IgG was used to label calreticulin. Images were acquired through a SPOT cooled color digital camera (Diagnostic Instruments Inc., Sterling Heights, MI).

Transmission Electron Microscopy and Immunoelectron Microscopy

Washed ejaculated sperm were adjusted to 5 × 10^6 sperm per 1.8-ml microfuge tube and then centrifuged at 4000 × g for 2 min to obtain a pellet. The pellet was fixed in 2.5% glutaraldehyde in 0.1 M cacodylate buffer (pH 7.4), postfixed with 1% OsO_4, dehydrated through a graded series of ethanol solutions to 100% ethanol, and embedded in LR white embedding medium. Thin sections (80 nm) were cut on a Reichert ultramicrotome and stained with uranyl acetate and lead citrate. All specimens were examined in a Philips 201 transmission electron microscope (Philips, New York, NY) at 80 kV.

For electron microscopic immunolocalization, sperm were fixed with 4% paraformaldehyde and 0.2% glutaraldehyde for 15 min and dehydrated through a graded series of ethanol solutions to 100% ethanol. The cells were infiltrated with and embedded in LR gold, which was polymerized by UV light for 24 h at −20°C. Thin sections were blocked with 5% normal goat serum and 3% BSA in PBS, then probed with anti-IP_3 receptor polyclonal antibody overnight at 4°C. After washing in PBS, sections were incubated for 1 h at room temperature with 10 nm gold-conjugated secondary antibody, goat anti-rabbit IgG. The sections were washed with distilled water and stained with uranyl acetate and lead citrate before examination.

Ca^{2+} and NADH Measurement (Fluorometry)

Washed sperm were adjusted to 10^7 sperm/ml with TALP and loaded with 5 μM fluorescence Ca^{2+} indicator fluo-3FF/AM ester for 40 min at 39°C. Extracellular dye was removed by centrifugation for 10 min at 170 × g. Sperm were resuspended in medium at 10^7/ml and incubated for an additional 20 min at 39°C to allow de-esterification of the fluo-3FF/AM ester to its membrane-impermeant, Ca^{2+}-sensitive form fluo-3FF. A 3-ml sperm suspension was added to each acrylic cuvette, maintained at 37–39°C, and constantly stirred. Hyperactivation was then induced as previously described [4] by 10 μM thapsigargin in TALP. TALP with 0.1% dimethyl sulfoxide (DMSO) was added to control samples because thapsigargin was first dissolved in DMSO and stored as stock solutions at −20°C. Fluorescence was monitored at 530 nm for Ca^{2+} (excitation at 490 nm) and 440 nm for NADH autofluorescence (excitation at 360 nm) with a Perkin-Elmer LS-5 fluorescence spectrophotometer. Samples (10 μl) were taken from the cuvettes, placed on slides, and evaluated at 200× for motility and hyperactivation.

ATP Extraction and Measurement

Hyperactivation was induced by treating 40 × 10^6 sperm/ml with 5 mM procaine for 5 min [19]. Extraction of sperm adenylate nucleotides (ATP, ADP, and AMP) was achieved by adding a 0.1-ml sperm suspension into test tubes containing 0.4 ml boiling water, boiling for 10 min, transferring to an ice bath, and centrifuging at 5000 × g for 30 min at 4°C. The supernatant was used for determination of ATP, ADP, and AMP. The pellet was saved and the sperm concentration was reevaluated using a hemocytometer. ADP was converted to ATP for measurement by incubating samples with 0.1 mM phosphoenolpyruvate and 0.08 mg/ml pyruvate kinase at 30°C for 30 min. AMP was converted to ATP by incubating samples with 0.1 mM phosphoenolpyruvate, 0.08 mg/ml pyruvate kinase, and 0.1 mg/ml myokinase at 30°C for 90 min [20]. ATP was determined using a luciferase reaction kit according to the manufacturer's protocol (ATP assay kit; Calbiochem). Bioluminescence was measured with a Berthold Lumat luminometer (Model LB 9501; Perkin-Elmer, Inc., Boston, MA) after addition of 100 μl luciferin-luciferase reagent. Light emission was calibrated using standard solutions of ATP.

CGP-37157 Treatment and Motility Analysis

CGP-37157 was dissolved in DMSO and aliquots were stored frozen at −20°C. The working solution was prepared immediately before addition to the sperm suspension by diluting the stock solution in TALP. The highest CGP-37157 concentration used in this study contained 0.05% DMSO; therefore, the solvent control was 0.05% DMSO in TALP.

Hyperactivation was induced by treating the sperm with 5 mM procaine [19]. Samples were taken for videotaping immediately after addition of CGP-37157 to sperm treated for 5 min with 5 mM procaine and immediately after addition of 5 mM procaine to sperm that had been pretreated for 5 min with CGP-37157. Sperm were videotaped using differential interference contrast at 320× magnification for 2 min per treatment. Videotapes were reviewed and the percentage of sperm exhibiting hyperactivated motility (% hyperactivation) was determined by categorizing 200 motile sperm for each treatment. Sperm exhibiting asymmetrical flagellar bending with circular or figure-of-eight trajectories [4, 16] were categorized as hyperactivated. In bull sperm, hyperactivation is a distinctive movement pattern, readily discriminated from the movement pattern of freshly ejaculated bull sperm. Percent motility was determined by categorizing 200 sperm as motile or immotile.

Statistical Analysis

All experiments were repeated at least three times using sperm samples collected from different bulls. Data are expressed as means ± SEM and were analyzed using Minitab statistical software (Minitab Inc., State College, PA). One-way analysis of variance (ANOVA) followed by Tukey pairwise comparisons was used to test for statistically significant differences among treatment groups, with $P < 0.05$ considered significant.

RESULTS

During spermiogenesis in placental mammals, all nuclear pores are moved to the RNE as the nucleus condenses [6, 9]. Therefore, to determine whether the RNE is the intracellular Ca^{2+} store in the neck region that initiates hy-
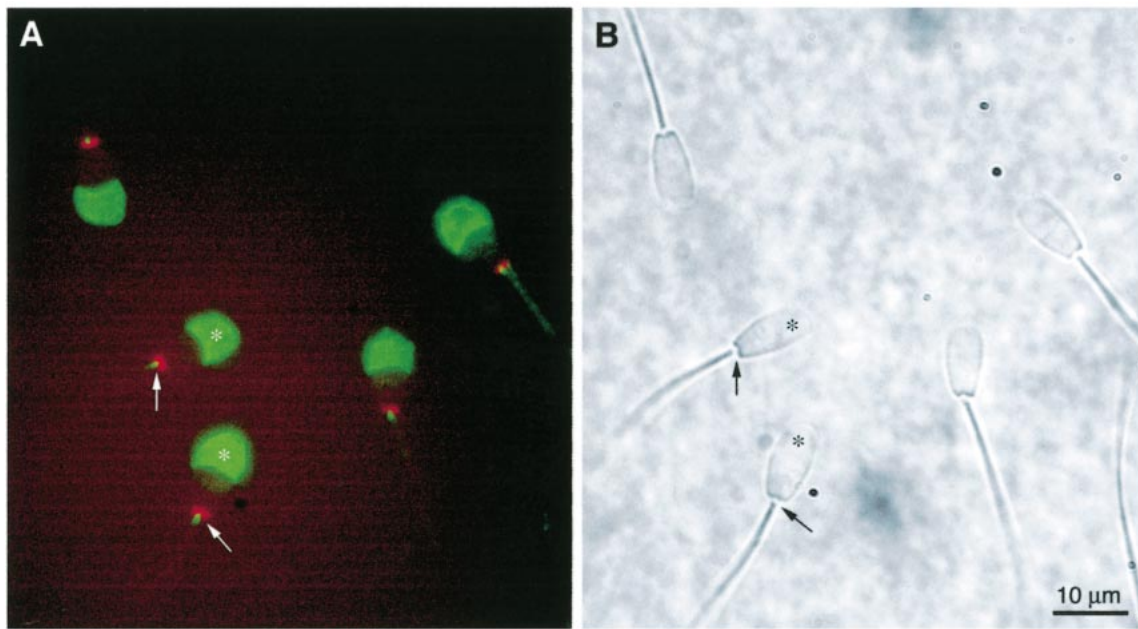
FIG. 1. Colocalization of nuclear pore complex proteins and IP$_3$ receptors. **A**) Nuclear pore complex proteins labeled with mAb 414 antibody were visualized by TRITC-conjugated secondary antibody, shown in red; IP$_3$ receptor labeling was visualized by FITC-conjugated secondary antibody, shown in green. IP$_3$ receptors localized at the acrosome (*) and the neck region (arrows) of sperm. Both the nuclear pore complex proteins and IP$_3$ receptors are localized to the neck region but do not completely overlap. **B**) Corresponding phase-contrast image of **A**.

peractivated motility, antinuclear pore complex antibody was used to identify RNE in bovine sperm. Anti-IP$_3$ receptor antibody was used to localize the IP$_3$ receptor-gated store in the sperm neck region. Both antibodies labeled areas in the neck region; however, the two labeled areas did not overlap entirely. The nuclear pores localized to a narrow band on the neck, while the IP$_3$ receptors localized to a central region in the neck, as seen when looking at the broad surface of the sperm head, and fluorescence extended further down the tail than the nuclear pore label (Fig. 1).

To explain the lack of complete overlap, transmission electron microscopy was used to study the ultrastructure of the sperm neck region in greater detail. When sections were cut through neck regions in the area labeled by antibody to nuclear pores, membranes enriched with nuclear pores were found (Fig. 2A). However, when sections were cut through neck regions labeled primarily by anti-IP$_3$ receptor, extensive membranous structures with enlarged cisternae or vesicles and few nuclear pores were found (Fig. 2, B and C). Immunoelectron microscopy was performed to identify the structure containing IP$_3$ receptor in sperm. The elaborate membranous structures of the RNE were not well preserved; however, specific deposition of gold particles was found in the region of the enlarged cisternae and vesicles. No mitochondria were labeled with anti-IP$_3$ receptor antibody (Fig. 3). Labeling of acrosomes served as a positive control (Fig. 3E) because acrosomes had been demonstrated to be IP$_3$ receptor-gated Ca^{2+} stores [21].

Calreticulin is a high-capacity Ca^{2+}-binding protein that is abundant within reticular Ca^{2+} stores [22]. In the bull sperm, calreticulin was detected in the acrosome and neck region where IP$_3$ receptors localized as well as in the principal piece of the tail (Fig. 4).

The response of mitochondria to induction of Ca^{2+} release and subsequent hyperactivation was assayed by measuring ATP and NADH. Sperm treated with 5 mM procaine hyperactivated within minutes. By 5 min, nearly 100% of motile sperm were hyperactivated. Incidence of hyperacti-

vation in control sperm was <1%. In procaine-treated sperm, ATP concentration was lower, ADP concentration was higher, and AMP concentration was the same as in control sperm (Fig. 5). This indicates that net ATP consumption was greater in hyperactivated than nonhyperactivated sperm. When sperm were hyperactivated with 10 μM thapsigargin as previously described [4], intracellular Ca^{2+} increased immediately, but no increase of NADH fluorescence could be detected (Fig. 6A), indicating that mitochondrial respiratory activity was not up-regulated when Ca^{2+} was released from the store. Addition of rotenone, an inhibitor of NADH oxidation, increased NADH fluorescence intensity, thereby demonstrating the ability to detect NADH increases in sperm (Fig. 6B).

Although mitochondria did not respond to induction of hyperactivation by increasing respiratory activity, they could play a role in turning on hyperactivation by releasing absorbed Ca^{2+} to the axoneme. Mitochondria release Ca^{2+} principally via a Na$^+$/Ca^{2+} exchanger located on the inner membrane. When CGP-37157, a specific blocker of the Na$^+$/Ca^{2+} exchanger [23], was applied before or after sperm were induced to hyperactivate by procaine, no effect was observed on the initial percentage of sperm that were hyperactivated nor on the percent of motile sperm (Fig. 7). However, 15 min after treatment with CGP-37157, there was a dose-dependent decrease in the percentage of motile sperm (Fig. 7, inset) and most of the sperm that remained motile at this time were very sluggish while others were arrested in a curved position. Nevertheless, asymmetrical flagellar beating was maintained until the flagella arrested.

DISCUSSION

Sperm are highly polarized and compartmentalized cells. One Ca^{2+} store, the acrosome, has been identified in the rostral sperm head by Walensky and Snyder [21] and has been demonstrated to play a role in acrosomal exocytosis. We propose that, in the tail, a compartment of the RNE
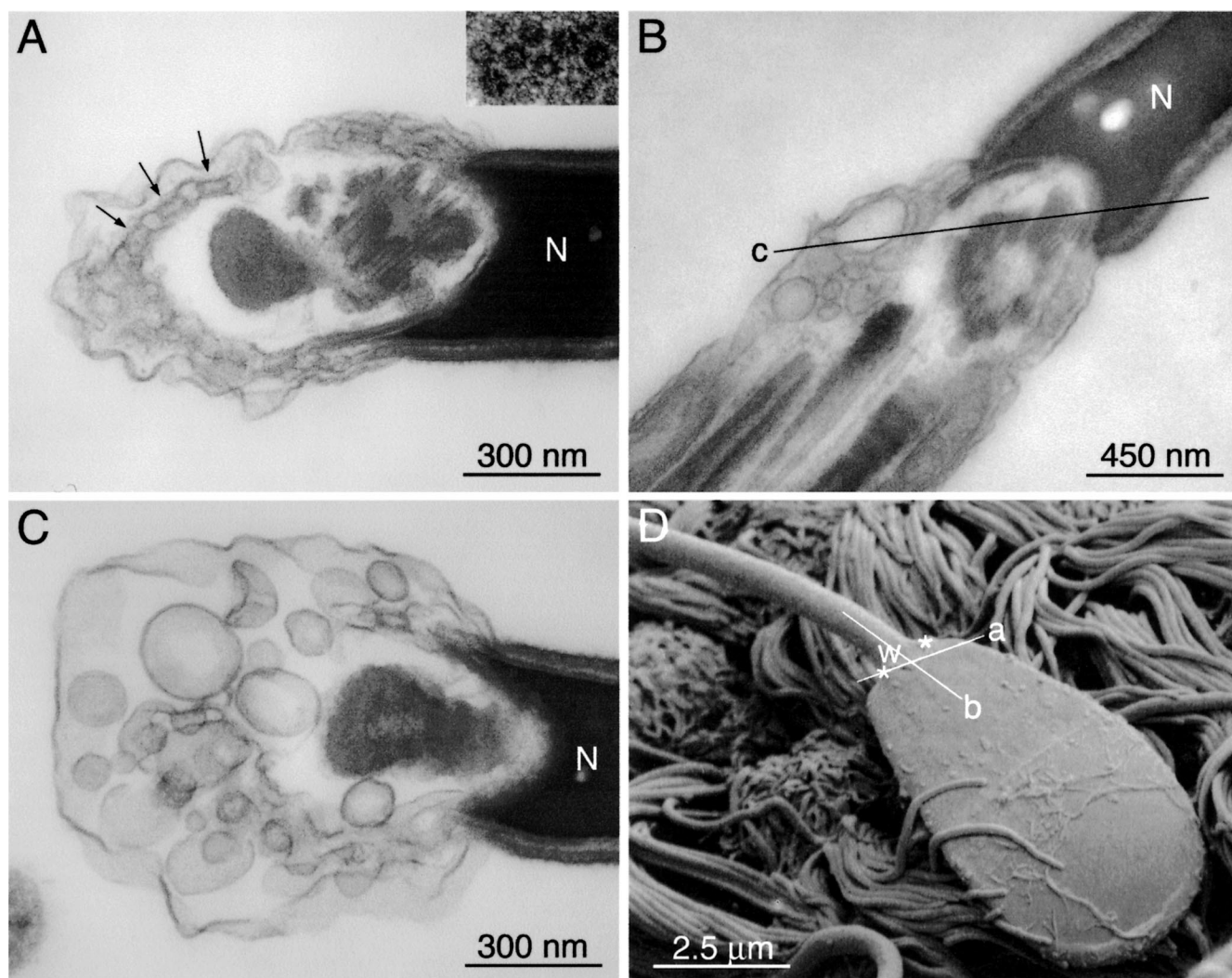
FIG. 2. Ultrastructure of the neck region of bull sperm. **A**) Transmission electron micrograph of the RNE region that is enriched with nuclear pores (see **D**, section line **a**). Arrows indicate nuclear pores. A tangent section through the membranes containing nuclear pores shows nuclear pores en face (inset). **B**) Transmission electron micrograph of the RNE region showing enlarged cisternae and vesicles (see **D**, section line **b**). **C**) Transmission electron micrograph of a different view of the enlarged cisternae and vesicles (see **B**, section line **c**) shows extensive vesicular structures. **D**) Scanning electron micrograph of bull sperm [35] with labels indicating location of membranes with nuclear pores (*) and region of enlarged cisternae (♦). (Scanning electron micrograph used with permission from S. Karger AG, Basel.) N, Nucleus.

serves as another intracellular Ca^{2+} store, one that is responsible for initiating hyperactivated motility.

The RNE is the excess nuclear envelope that arises as the result of chromatin condensation during spermiogenesis. The nuclear envelope is drawn into the region of the developing tail as nuclear volume decreases [6]. It eventually forms a scroll in a restricted region of the neck, next to the base of the proximal centriole and the most proximal of the mitochondria [8]. The RNE is closely associated with these mitochondria, where it sits between the plasma membrane and axoneme. Previously, we detected IP_3 receptors in the neck region [4]. In the present study, we further determined that IP_3 receptors are localized to membranous structures in the neck region that contain enlarged cisternae and few nuclear pores. We speculate that these enlarged cisternae are a specialized subcompartment of the RNE because there have been no reports of retention of ER in fully mature sperm after expulsion of the cytoplasmic droplet. Nevertheless, we cannot completely rule out the possibility that these membranous structures are remnants of ER or even Golgi. Nuclear envelopes, ER, and Golgi have all

been identified as Ca^{2+} stores in other cell types [11, 12, 24].

Calreticulin, the major Ca^{2+}-binding protein in Ca^{2+} stores, was also localized to the neck region of the bull sperm. Because both antibodies were raised in rabbits, no colocalization was performed here for IP_3 receptors and calreticulin. However, in human sperm, calreticulin and IP_3 receptors have been colocalized to vesicular structures in the neck region [25]. In addition, a high concentration of calmodulin has also been detected in the base of the flagellum in several species [26, 27]. These data indicate that the RNE serves as the intracellular Ca^{2+} store that is responsible for releasing Ca^{2+} to initiate hyperactivated motility in mammalian sperm.

Besides acrosome and the neck region of sperm, calreticulin also localized to the principal piece, where no IP_3 receptor was detected. Calreticulin has also been found in the cytosol not associated with membranes or Ca^{2+} stores in other cell types, although the function has yet to be determined [22].

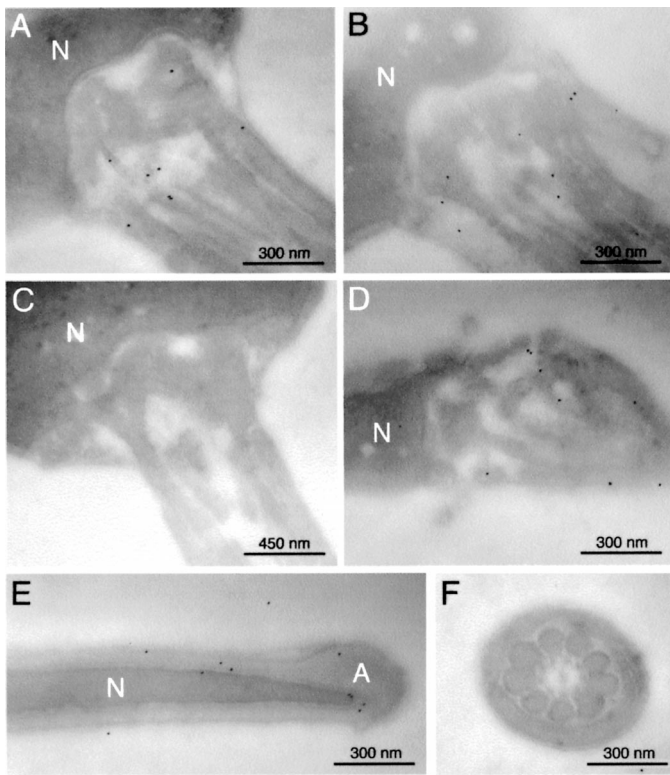The mitochondria of mammalian sperm are restricted to

FIG. 3. Localization of IP$_3$ receptors by immunogold labeling. **A**, **B**, **D**) Antibody to IP$_3$ receptor localized to the region of the neck in which enlarged cisternae were seen. **C**) Control section incubated with preimmune serum showed no labeling in the same region. **E**) IP$_3$ receptors were also found in the acrosomal region as predicted. **F**) No labeling could be found in mitochondria. A, Acrosome; N, nucleus.

the flagellar midpiece. They wrap tightly in a helical fashion around the axoneme and outer dense fibers of the flagellum and can therefore provide ATP to the dynein ATPase in the midpiece axoneme [5, 28]. Ca^{2+} is a well-known activator of mitochondrial dehydrogenases [15]. The activation of mitochondrial dehydrogenases can, in turn, increase ATP production. Increases in cytosolic Ca^{2+} have been shown to produce increases in mitochondrial Ca^{2+}, which then stimulate oxidative metabolism [23, 29]. The coupling between increases in cytosolic and mitochondrial
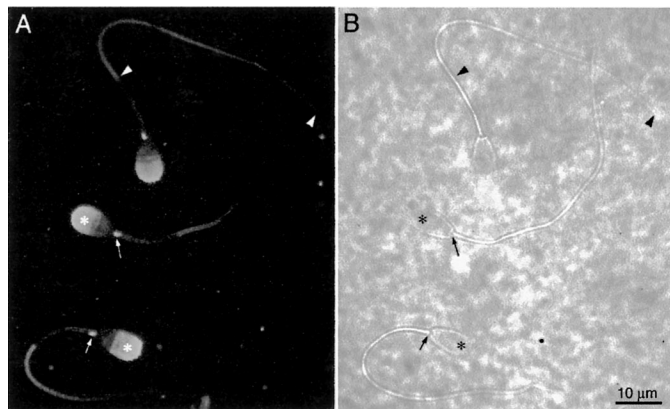

FIG. 4. Localization of calreticulin in bull sperm. **A**) Calreticulin was localized in the neck region (arrows) where IP$_3$ receptors had been localized. The labeling was also found in the acrosomes (*) and principal piece (between arrowheads). **B**) Corresponding phase-contrast image of **A**.
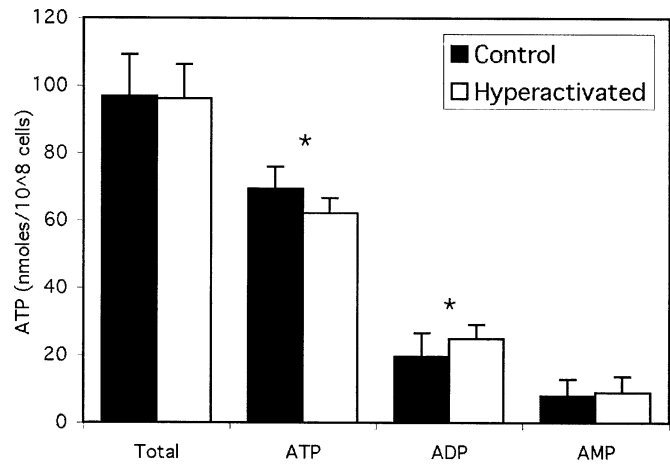

FIG. 5. Concentrations of adenylate nucleotides in nonhyperactivated (filled bars) and hyperactivated (open bars) sperm. Bull sperm hyperactivated with 5 mM procaine for 5 min contained significantly less ATP and more ADP than nonhyperactivated, control sperm (*, $P < 0.05$), although the AMP and total adenylate nucleotides are not different ($P > 0.05$, n = 5 bulls).

Ca^{2+} has been proposed to coordinate mitochondrial ATP production with cellular energy demand [15]. In demembranated bull sperm, higher levels of ATP were required to support hyperactivated than nonhyperactivated motility [16]. In the present study, we found that hyperactivated bull sperm did consume more ATP than nonhyperactivated sperm and the decreased ATP/ADP ratio in hyperactivated sperm indicated increased energy metabolism. Nevertheless, we did not detect increased NADH in hyperactivated sperm, indicating that mitochondrial energy production is not increased during induction of hyperactivation. Decrease in intracellular ATP concentration has also been associated with the appearance of hyperactivated motility in rat sperm [30]. In contrast, ATP concentration was 2-fold higher in hyperactivated than nonhyperactivated guinea-pig sperm [19]; however, glucose was present in the medium and therefore the additional ATP could have been produced by glycolysis instead of oxidative phosphorylation.

Because we did not see an increase in mitochondrial activity, we asked whether there is enough ATP present to support the increased demands of hyperactivation [16]. In this study, the total amount of ATP in bull sperm was estimated to be around 20 mM. This was considerably higher than the 2 mM of ATP required to hyperactivate demembranated bull sperm [16]. Sperm are known to possess very high ATP content compared with other cells (rat sperm: 15
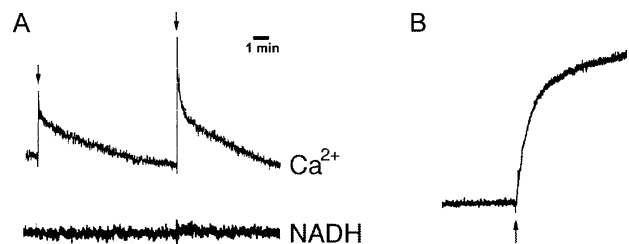

FIG. 6. Fluorometric measurement of mitochondrial NADH activity. **A**) Mitochondrial NADH activity in thapsigargin-induced hyperactivated sperm. Sperm hyperactivated with 10 μM thapsigargin (arrows) showed an immediate increase in intracellular Ca^{2+} concentration; however, the mitochondrial NADH autofluorescence remained unchanged when Ca^{2+} increased. **B**) Mitochondrial NADH increased when 0.1 μM rotenone was added as a positive control (arrow).
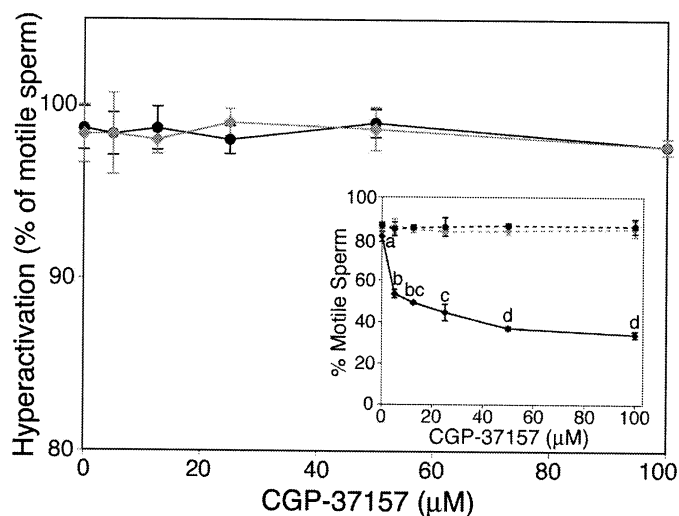
FIG. 7. Effect of CGP-37157 on hyperactivated motility. CGP-37157 was added before (●) or after (♦) sperm were hyperactivated by 5 mM procaine; no difference in percent hyperactivation and percent motility (inset, dashed lines) was detected immediately after treatment ($P > 0.05$, n = 3 bulls). Percent motile sperm evaluated 15 min after treatment decreased when CGP-37157 was increased (inset, solid line). Means with different letters are significantly different ($P < 0.05$).

mM [30]; hepatocytes: 2 mM [31]). High levels of ATP are presumably synthesized in sperm by a respiration-coupled process during epididymal transit [32]. Epididymal rat sperm suspended in substrate-free medium remained as motile as sperm suspended in medium with metabolic substrates for at least 90 min [30]. Thus, the increased ATP demand of hyperactivation may be met, at least initially, by hydrolyzing more ATP from reserves instead of by producing more ATP from oxidative respiration.

The benzothiazepine CGP-37157 selectively and potently inhibits the Na^+/Ca^{2+} exchanger that exports Ca^{2+} from isolated heart mitochondria [33, 34]. It reversibly slows the mitochondrial Ca^{2+} fall in chromaffin cells [23]. CGP-37157 is a lipophilic compound and is expected to cross the plasma membrane easily. We applied CGP-37157 before and after induction of hyperactivation by procaine to determine whether blocking release of Ca^{2+} from mitochondria could prevent hyperactivation. No immediate effects were observed when CGP-37157 was added either before or after induction of hyperactivation, indicating that Ca^{2+} could reach the axoneme without the mediation of mitochondria. Therefore, mitochondria in sperm might not have the role, as in other cell types, of fine-tuning Ca^{2+} signals by taking up Ca^{2+} released from stores and gradually releasing it to the cytosol (in this case, the cytosol surrounding the axoneme). In high doses or after prolonged incubation (>10 min), CGP-37157 did affect sperm motility by decreasing the number of motile sperm. Nevertheless, it did not affect flagellar beat asymmetry, which is characteristic of bull sperm hyperactivation and is dependent on Ca^{2+} [16].

This study has focused on the initiation of hyperactivation. Maintenance of hyperactivation for long periods may well require an influx of extracellular Ca^{2+} and/or activation of mitochondria.

We conclude that the Ca^{2+} store found in the neck region of sperm is located in the enlarged cisternae that may be derived from the RNE. The Ca^{2+} released from the store seems to affect the axoneme directly, without intervention of mitochondria. Mitochondrial respiration does not appear to be up-regulated by the released Ca^{2+}.

REFERENCES

1. Katz DF, Yanagimachi R. Movement characteristics of hamster spermatozoa within the oviduct. Biol Reprod 1980; 22:759–764.
2. Suarez SS, Osman RA. Initiation of hyperactivated flagellar bending in mouse sperm within the female reproductive tract. Biol Reprod 1987; 36:1191–1198.
3. Yanagimachi R. Mammalian fertilization. In: Knobil E, Neill J (eds.), The Physiology of Reproduction. New York: Raven Press; 1994: 189–317.
4. Ho H-C, Suarez SS. An inositol 1,4,5-trisphosphate receptor-gated intracellular Ca^{2+} store is involved in regulating sperm hyperactivated motility. Biol Reprod 2001; 65:1606–1615.
5. Fawcett DW. The mammalian spermatozoon. Dev Biol 1975; 44:394–436.
6. Franklin LE. Formation of the redundant nuclear envelope in monkey spermatids. Anat Rec 1968; 161:149–162.
7. Toshimori K, Higashi R, Oura C. Distribution of intramembranous particles and filipin-sterol complexes in mouse sperm membranes: polyene antibiotic filipin treatment. Am J Anat 1985; 174:455–470.
8. Rouse GW, Robson SK. An ultrastructural study of megachiropteran (Mammalia: Chiroptera) spermatozoa: implications for chiropteran phylogeny. J Submicrosc Cytol 1986; 18:137–152.
9. Oko RJ, Costerton JW, Coulter GH. An ultrastructural study of the head region of bovine spermatozoa. Can J Zool 1976; 54:1326–1340.
10. Kerr JB. Ultrastructure of the seminiferous epithelium and intertubular tissue of the human testis. J Electron Microsc Tech 1991; 19:215–240.
11. Gerasimenko OV, Gerasimenko JV, Tepikin AV, Petersen OH. ATP-dependent accumulation and inositol trisphosphate- or cyclic ADP-ribose-mediated release of Ca^{2+} from the nuclear envelope. Cell 1995; 80:439–444.
12. Santella L, Kyozuka K. Effects of 1-methyladenine on nuclear Ca^{2+} transients and meiosis resumption in starfish oocytes are mimicked by the nuclear injection of inositol 1,4,5-trisphosphate and cADP-ribose. Cell Calcium 1997; 22:11–20.
13. Robb-Gaspers LD, Rutter GA, Burnett P, Hajnoczky G, Denton RM, Thomas AP. Coupling between cytosolic and mitochondrial calcium oscillations: role in the regulation of hepatic metabolism. Biochim Biophys Acta 1998; 1366:17–32.
14. Rizzuto R, Pinton P, Carrington W, Fay FS, Fogarty KE, Lifshitz LM, Tuft RA, Pozzan T. Close contacts with the endoplasmic reticulum as determinants of mitochondrial Ca^{2+} responses. Science 1998; 280: 1763–1766.
15. McCormack JG, Halestrap AP, Denton RM. Role of calcium ions in regulation of mammalian intramitochondrial metabolism. Physiol Rev 1990; 70:391–425.
16. Ho H-C, Granish KA, Suarez SS. Hyperactivated motility of bull sperm is triggered at the axoneme by Ca^{2+} and not cAMP. Dev Biol 2002; 250:208–217.
17. Parys JB, de Smedt H, Missiaen L, Bootman MD, Sienaert I, Casteels R. Rat basophilic leukemia cells as model system for inositol 1,4,5-trisphosphate receptor IV, a receptor of the type II family: functional comparison and immunological detection. Cell Calcium 1995; 17: 239–249.
18. Meier E, Miller BR, Forbes DJ. Nuclear pore complex assembly studied with a biochemical assay for annulate lamellae formation. J Cell Biol 1995; 129:1459–1472.
19. Mujica A, Neri-Bazan L, Tash JS, Uribe S. Mechanism for procaine-mediated hyperactivated motility in guinea pig spermatozoa. Mol Reprod Dev 1994; 38:285–292.
20. Ford SR, Leach FR. Bioluminescent assay of the adenylate energy charge. Methods Mol Biol 1998; 102:69–81.
21. Walensky LD, Snyder SH. Inositol 1,4,5-trisphosphate receptors selectively localized to the acrosomes of mammalian sperm. J Cell Biol 1995; 130:857–869.

22. Krause KH, Michalak M. Calreticulin. Cell 1997; 88:439–443.
23. Babcock DF, Herrington J, Goodwin PC, Park YB, Hille B. Mitochondrial participation in the intracellular Ca^{2+} network. J Cell Biol 1997; 136:833–844.
24. Pinton P, Pozzan T, Rizzuto R. The Golgi apparatus is an inositol 1,4,5-trisphosphate-sensitive Ca^{2+} store, with functional properties distinct from those of the endoplasmic reticulum. EMBO J 1998; 17: 5298–5308.
25. Naaby-Hansen S, Wolkowicz MJ, Klotz K, Bush LA, Westbrook VA, Shibahara H, Shetty J, Coonrod SA, Reddi PP, Shannon J, Kinter M, Sherman NE, Fox J, Flickinger CJ, Herr JC. Co-localization of the inositol 1,4,5-trisphosphate receptor and calreticulin in the equatorial segment and in membrane bounded vesicles in the cytoplasmic droplet of human spermatozoa. Mol Hum Reprod 2001; 7:923–933.
26. Jones HP, Lenz RW, Palevitz BA, Cormier MJ. Calmodulin localization in mammalian spermatozoa. Proc Natl Acad Sci U S A 1980; 77: 2772–2776.
27. Feinberg J, Weinman J, Weinman S, Walsh MP, Harricane MC, Gabrion J, Demaille JG. Immunocytochemical and biochemical evidence for the presence of calmodulin in bull sperm flagellum. Biochim Biophys Acta 1981; 673:303–311.
28. Phillips DM. Mitochondrial disposition in mammalian spermatozoa. J Ultrastruct Res 1977; 2:144–154.
29. Hajnoczky G, Robb-Gaspers LD, Seitz MB, Thomas AP. Decoding of cytosolic calcium oscillations in the mitochondria. Cell 1995; 82:415–424.
30. Jeulin C, Soufir J-C. Reversible intracellular ATP changes in intact rat spermatozoa and effects on flagellar sperm movement. Cell Motil Cytoskeleton 1992; 21:201–222.
31. Fladmark KE, Brustugun OT, Mellgren G, Krakstad C, Boe R, Vintermyr OK, Schulman H, Doskeland SO. Ca^{2+}/calmodulin-dependent protein kinase II is required for microcystin-induced apoptosis. J Biol Chem 2002; 277:2804–2811.
32. Cooper TG. Sperm energy metabolism. In: Cooper TG (ed.), The Epididymis, Sperm Maturation and Fertilization. Berlin, Heidelberg: Springer-Verlag; 1986: 14–15.
33. Cox DA, Conforti L, Sperelakis N, Matlib MA. Selectivity of inhibition of Na^+-Ca^{2+} exchange of heart mitochondria by benzothiazepine CGP-37157. J Cardiovasc Pharmacol 1993: 21:595–599.
34. Cox DA, Matlib MA. A role for the mitochondrial Na^+-Ca^{2+} exchanger in the regulation of oxidative phosphorylation in isolated heart mitochondria. J Biol Chem 1993; 268:938–947.
35. Suarez SS. Carbohydrate-mediated formation of the oviductal sperm reservoir in mammals. Cells Tissues Organs 2001; 168:105–112.